World Scientific Research Journal Volume 11 Issue 4, 2025
ISSN: 2472-3703 DOI: 10.6911/WSRJ.202504_11(4).0015

Recent Advances in the Structure, Properties, and Applications of Lead-Free Tin-Based Perovskites in Optoelectronic Devices

Shuo Wang, Huixin Xiu

School of materials and chemistry, University of Shanghai for Science and Technology,
Shanghai, China

Abstract

In recent years, metal halide perovskites (MHPs) have emerged as a research hotspot in optoelectronic devices due to their exceptional optoelectronic properties. However, the environmental toxicity of commonly used lead halide perovskites (LHPs) has prompted researchers to explore alternative lead-free perovskite materials. Among these, tin halide perovskites (THPs), which exhibit structural and performance similarities to LHPs, have become the most significant focus in the study of lead-free perovskites. This review comprehensively summarizes the types, structural characteristics, defect mechanisms, and recent research progress of lead-free tin-based perovskites in optoelectronic devices. First, the typical tin-based perovskite material systems, including $FASnX_3$, $MASnX_3$, and $CsSnX_3$, are introduced. Subsequently, their optoelectronic properties, defect types, and environmental stability issues are discussed, with a particular emphasis on their applications and optimization strategies in perovskites solar cells (PSCs), photodetectors (PDs), and light-emitting diodes (LEDs). These strategies include defect passivation, stabilization through additives, interface engineering and energy level modulation of hole transport layers (HTLs) and electron transport layers (ETLs), as well as structural optimization and research on low-dimensional nanostructured perovskites. Finally, the current challenges faced by tin-based perovskites are analyzed, and their future development directions toward highly efficient and stable optoelectronic devices are prospected.

Keywords

Lead-free tin-Based perovskites; Environmental stability; Solar cells; Photodetectors; Light-emitting diodes.

1. INTRODUCTION

In 1893, the German scientist Gustav Rose discovered $CaTiO_3$ in the Ural Mountains of Russia and called it a new name "perovskite" in honor of the Russian mineralogist Count Lev Perovski [1]. Metal halide perovskites have emerged as promising candidates for future photovoltaic and optoelectronic applications, such as solar cells, light-emitting diodes, and photodetectors, owing to their exceptional optoelectronic properties[13; 23; 44]. These include high light absorption coefficients, high charge carrier mobility, long photogenerated carrier lifetimes, low exciton binding energies, and tunable bandgaps[25; 30].

Among the family of metal halide perovskites, lead halide perovskites have been the most studied materials. However, the toxic degradation byproducts of lead-based perovskites pose significant environmental risks, potentially harming ecosystems. Consequently, research focus has gradually shifted toward more environmentally friendly lead-free perovskite alternatives [7; 16; 48].

While lead-based perovskites are considered ideal materials for sustainable energy applications due to their balance between efficiency and cost, lead-free perovskites are regarded as the next-generation optoelectronic materials with the potential to revolutionize the field. The first tin-based perovskite was successfully synthesized by Fisher et al.[37]in 1974, followed by Yamada et al., who introduced the first hybrid THP. These pioneering studies have significantly spurred widespread scientific interest and in-depth exploration of THP-based devices [50; 51].

Due to the similar ionic radii of tin (Sn) and lead (Pb) (Sn: 110 pm, Pb: 119 pm) and their analogous valence electron configurations (ns^2np^2), Sn has been predicted as a natural substitute for Pb[2; 19]. Like Pb, Sn also possesses inactive outer orbitals, a characteristic crucial for achieving the unique electrical and optical properties of MHPs. However, the performance and stability of tin-based perovskite solar cells are significantly constrained by the tendency of Sn^{2+} to oxidize to Sn^{4+} under ambient conditions, as well as the high prevalence of Sn vacancy defects[20]. These factors contribute to the rapid degradation of tin-based perovskite materials, resulting in optoelectronic devices based on Sn significantly underperforming compared to their Pb-based counterparts. Currently, most research focuses on polycrystalline thin films, which often contain numerous grain boundaries and associated defects. These defects can trap charges and enhance non-radiative recombination, thereby substantially limiting the improvement of device performance [39; 47].

This review focuses on the main types of tin-based halide perovskites, the mechanisms underlying their environmental stability, and the latest advancements in solar cells, photodetectors, and light-emitting diodes.

2. STRUCTURE AND BASIC PROPERTIES

2.1. Structural characteristics

2.1.1 $FASnX_3$

THP mainly consists of three types: $FASnX_3$, $MASnX_3$, and $CsSnX_3$ (X = I, Br, Cl). Its crystal structure is influenced by temperature and ionic size, exhibiting different phase transition behaviors. For instance, $FASnX_3$ adopts a cubic structure, as illustrated in **Figure 1**. From the figure, it can be observed that the organic cation FA is consistently located at the center of the cubic framework, and the orientation of the C—N bond varies with the type of halogen atom. The Sn atoms are positioned at the edges of the cube and are coordinated octahedrally with halogen atoms. At room temperature, the orientation of FA molecules remains disordered. Due to the steric hindrance effect of the FA cation, the Sn—I bond length is measured at 3.158 Å, and $FASnI_3$ adopts a pseudo-cubic crystal structure at 340 K[39].

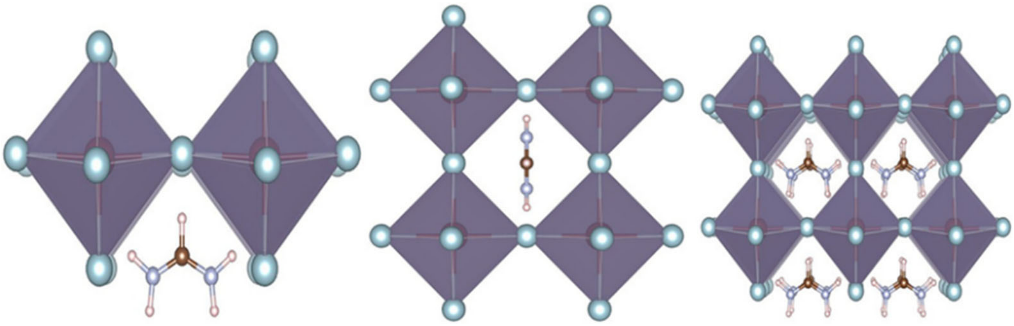

Figure 1. The polyhedral cubic perovskite 3D crystal structures of $FASnI_3$, $FASnBr_3$, and $FASnCl_3$ compounds[34]

2.1.2 $MASnX_3$

The structure of $MASnX_3$ perovskite is isomorphic to that of $FASnX_3$, as shown in Figure 2. At 295 K, it exists in a cubic phase but undergoes a phase transition to a lower-symmetry tetragonal phase at 275 K [40; 42]. Due to the tilting of SnI_6 octahedra around the vertical axis, the tetragonal structure can be regarded as an expanded supercell of the cubic lattice. When the temperature is further reduced to 108–114 K, another phase transition occurs from the tetragonal to the orthorhombic phase [24].In this orthorhombic phase, the SnI_6 octahedra tilt in the same direction around the c-axis within adjacent planes, and the cation arrangement becomes more rigid, restricting rotational freedom. This configuration leads to further localization of holes, thereby extending the carrier lifetime [35]. First-principles calculations suggest that this phase exhibits extremely low electrical conductivity, making it a candidate for low-temperature electronics and other potential applications in this field [22].

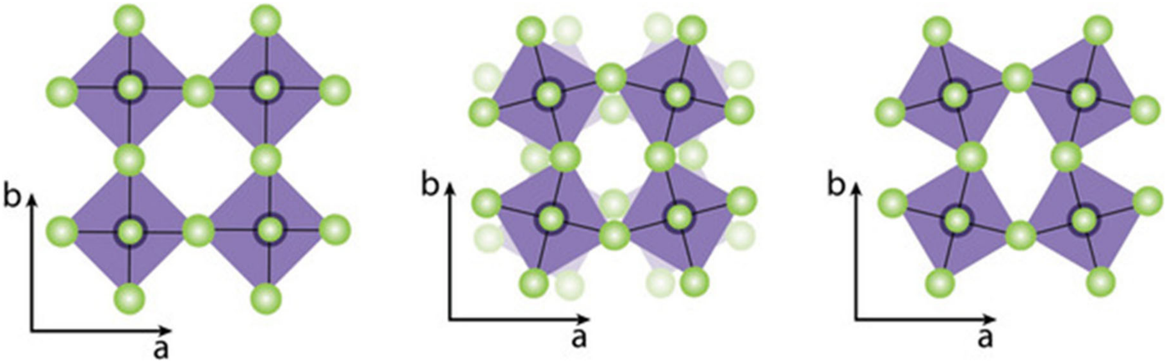

Figure 2. The adjacent octahedral layer of $MASnX_3$ rotates along the c-axis according to the crystal orientation[12]

2.1.3 $CsSnX_3$

For $CsSnX_3$, the smaller size of Cs^+ ions compared to MA^+ or FA^+ leads to significant rotation and tilting of the SnI_6 octahedra, thereby affecting the structural stability of $CsSnI_3$ at room temperature. At an elevated temperature of 500 K, $CsSnI_3$ perovskite adopts a black cubic phase. As the temperature decreases to 380 K, this cubic phase transitions into a lower-symmetry black tetragonal phase. Upon further cooling to 300 K, the tetragonal phase transforms into a black orthorhombic phase, which exhibits high stability at room temperature [9].Studies have shown that the black tetragonal phase of $CsSnI_3$ perovskite offers the best performance for device applications. However, this phase is prone to structural transformation when exposed to ambient air or organic solvents, leading to the formation of a double-chain structure, as illustrated in Figure 3(d). The formation of this double-chain structure is strongly influenced by moisture and oxygen in the air and is often accompanied by further degradation of the material into Cs_2SnI_6. Since Cs_2SnI_6 exhibits poor optoelectronic and electrical properties, it is unsuitable for high-performance applications such as photovoltaic devices and field effect transistors [33].

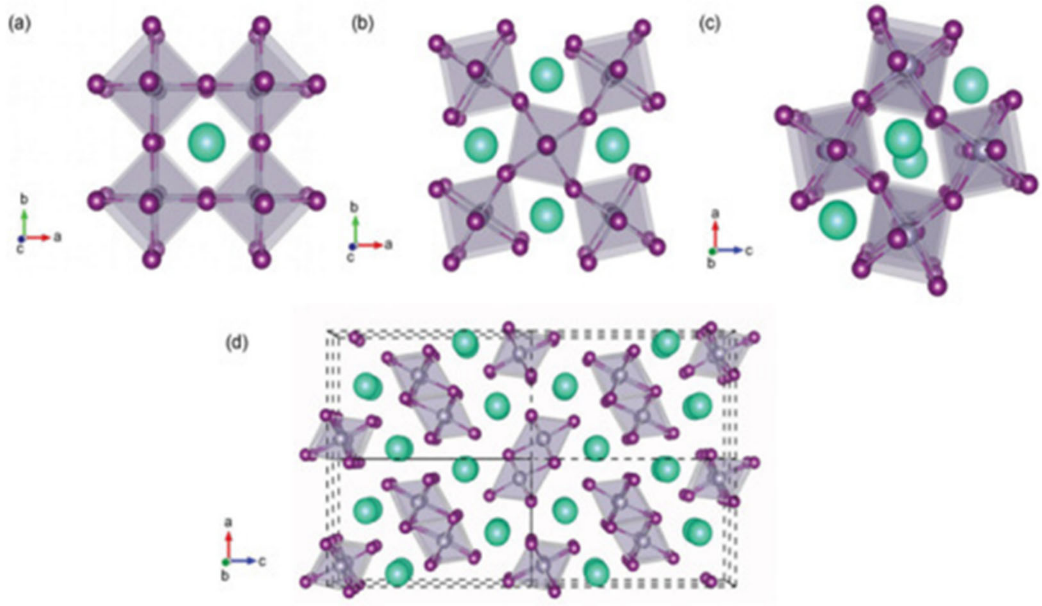

Figure 3. (a) Cubic $CsSnI_3$ perovskite (b) Tetragonal $CsSnI_3$ perovskite,(c) Orthogonal $CsSnI_3$ perovskite,(d) Cleavage and bonding of octahedral $CsSnI_3$ network[10]

2.2. Optoelectronic properties

2.2.1 Band structure

The bandgap of THP is slightly lower than that of lead-based materials, making it more suitable for near-infrared optoelectronic devices. To effectively utilize perovskite materials in optoelectronic applications, a key requirement is a widely tunable bandgap along with efficient light emission. The absorption spectrum provides insights into the electronic band structure and density of states, while the photoluminescence (PL) spectrum reveals critical optical properties such as emission peak position, emission characteristics, full width at half maximum (FWHM), defect states, and photoluminescence quantum yield (PLQY), all of which are fundamental for the successful application of perovskite single crystals.

Taking $CsSnX_3$ as an example, Figure 4(A) shows that Pb and Sn based materials exhibit similar direct bandgaps. As the halide ion radius increases (from Cl to I), the bandgap gradually decreases. Figure 4(B) presents the calculated DOS distributions for $CsSnCl_3$, $CsSnBr_3$, and $CsSnI_3$, indicating that the valence band maximum (VBM) primarily originates from the p-orbitals of halogen atoms, while the conduction band minimum (CBM) is mainly derived from the p-orbitals of Sn or Pb [55]. The bandgap is predominantly influenced by Sn/Pb and halide ions, with little dependence on organic cations [31].The incorporation of mixed halides with Pb and Sn significantly alters the band structure, introducing band bending, as shown in Figure 4(C). The partial density of states (PDOS) calculations for Sn, illustrated in Figure 4(D), show that as Sn concentration increases, the contribution of Sn 4p electrons to the conduction band minimum (CBM) also increases, while the energy level of the p-orbitals decreases[8].Further studies suggest that as Sn concentration increases, spin-orbit coupling and structural distortions also influence the absorption and photoluminescence (PL) peak positions [21].

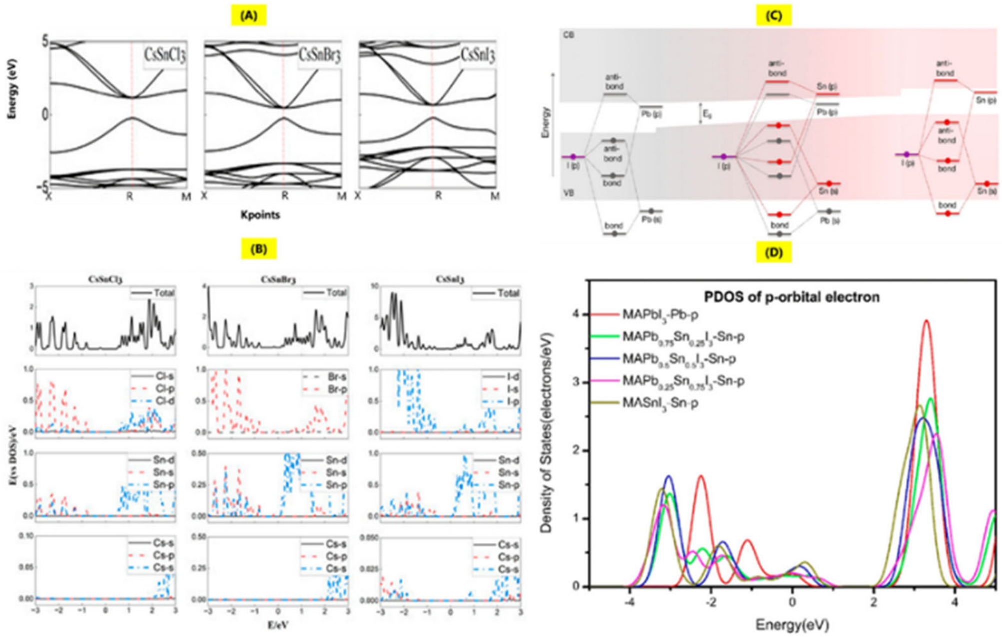

Figure 4. (A)-(B) Band structure of $CsSnCl_3$, $CsSnBr_3$, and $CsSnI_3$ and band bending in DOS (C) Hybrid halide perovskites (D) Skewness of p-orbital electrons in mixed halide perovskites[8; 17]

2.2.2 Carrier dynamics

The optoelectronic properties of all perovskites are dependent on their octahedral network. Substituting Pb with Sn reduces the bandgap, leading to redshifted emission. Therefore, understanding carrier dynamics is crucial for designing suitable materials for high-efficiency optoelectronic devices.

Similar to lead-based perovskites, the optical properties of THP can be tuned by adjusting its halide composition and crystal size. Dai et al. [11] reported the absorption and PL spectra of $FASnI_3$ nanocrystals (NCs) grown at different reaction temperatures (25 to 125 °C), with corresponding sizes ranging from 7.3 to 12.1 nm, as shown in Figure 5. For this size range, a broad spectral tunability from 650 to 750 nm is evident, highlighting the significant impact of NC size on charge carrier dynamics.

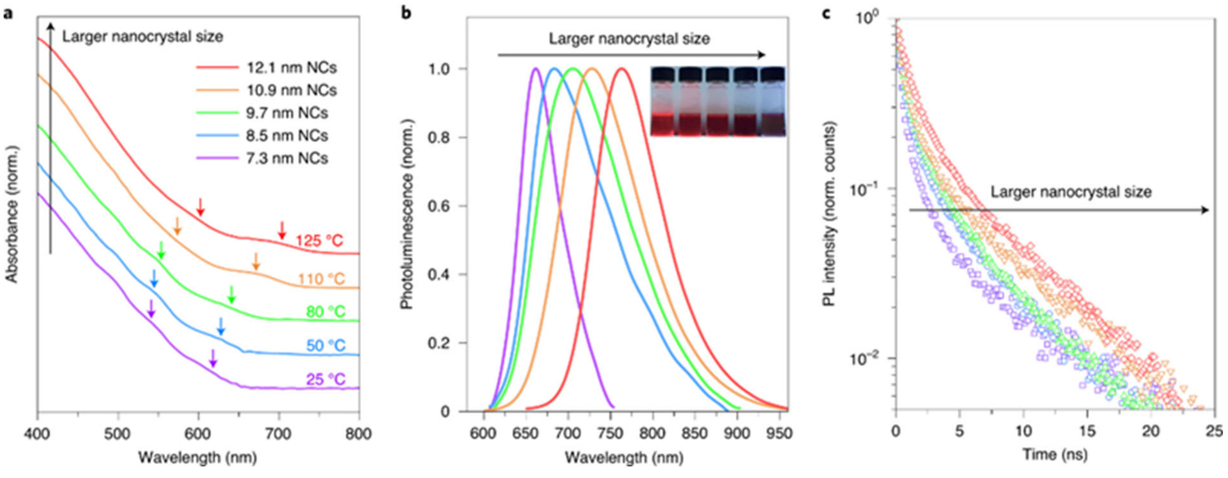

Figure 5. (a) Steady-state absorption spectra of FASnI3 NC at different growth temperatures (b) Steady-state PL spectra of FASnI3 NC (c) TRPL spectra of $FASnI_3$ NC

2.3. Defects in Perovskite

Defects in perovskite crystals have a significant impact on the performance of optoelectronic devices. Common types of defects include point defects, planar defects, grain boundary defects, bulk defects, and dislocations [38; 43; 45; 54], as illustrated in Figure 6.

Among these, point defects have been the most extensively studied. They can be categorized into three types of vacancies (VA, VB, VX), three types of interstitials (Ai, Bi, Xi), six types of antisite defects (AB, AX, BA, BX, XA, XB), and Frenkel defect pairs [4]. Surface and grain boundary defects arise due to the lower coordination number of surface ions compared to the bulk region, leading to local structural abnormalities. In tin-based and lead-tin hybrid perovskite thin films prepared via low-temperature solution processing, polycrystalline interfaces tend to form grain boundaries [14]. These grain boundaries are commonly observed in thin films composed of fine grains, leading to the presence of under-coordinated Sn atoms and a high density of trap states. The defects induced by grain boundaries significantly enhance nonradiative carrier recombination, thereby reducing the optoelectronic performance of the material [46]. Bulk defects primarily include voids, precipitates, and secondary phase domains, which induce structural, compositional, and density variations, resulting in changes in crystal volume and morphology[26]. Overall, nearly all types of defects can substantially alter the structural properties of the perovskite lattice, profoundly affecting the photovoltaic performance of solar cells, the detectivity of photodetectors, and the external quantum efficiency of LEDs.

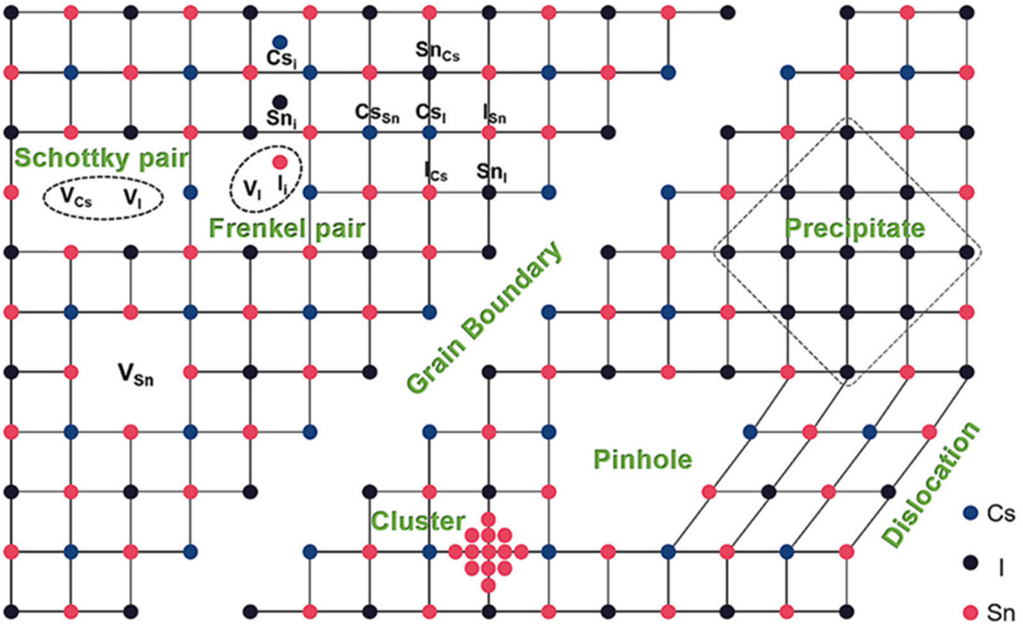

Figure 6. Schematic diagram of basic defect classification in tin-based perovskites ($CsSnI_3$) [5]

2.4. Environmental oxidation mechanism of tin-based perovskites

The oxidation of Sn^{2+} in tin-based perovskites is one of the most extensively studied issues in this field. In 2019, Zhang et al. [59] conducted further research and analysis to elucidate the intrinsic mechanism behind the oxidation of tin-based perovskites. They proposed that the fundamental reason for the susceptibility of tin-based perovskites to oxidation lies in the lack of a lanthanide contraction effect in tin (Sn) [3]. For lead (Pb), the lanthanide contraction causes the 6s electrons to be closer to the nucleus, resulting in a smaller atomic radius. In contrast, Sn lacks a significant lanthanide contraction effect due to its higher atomic energy levels, lower electronegativity, and smaller energy splitting between the s and p orbitals [41]. This absence of lanthanide contraction significantly reduces the ionization energy (the energy required to remove an electron) of Sn, making it energetically easier for Sn to lose its 5s electrons. This tendency increases the likelihood of vacancy defects and enhances the material's oxidation propensity.

Secondly, Sn vacancies are also considered a critical issue contributing to the oxidation of perovskites. Sn^{2+} is easily oxidized to Sn^{4+}, and the formation energy of Sn vacancies is generally lower than that of other types of point defects. As illustrated in Figure 7, Sn vacancies on the perovskite surface primarily act as non-radiative recombination centers. They capture electrons or holes, inhibiting their thermal excitation and ultimately causing annihilation with oppositely charged carriers. This results in non-radiative recombination, leading to significant voltage losses and a reduction in open-circuit voltage. Additionally, Sn vacancies within the bulk of the perovskite spontaneously convert into Sn, releasing two holes into the valence band and inducing p-type self-doping [32]. Severe p-type self-doping results in high background hole densities and high electron-hole recombination rates, significantly shortening the lifetime and diffusion length of photogenerated carriers, ultimately degrading device performance.

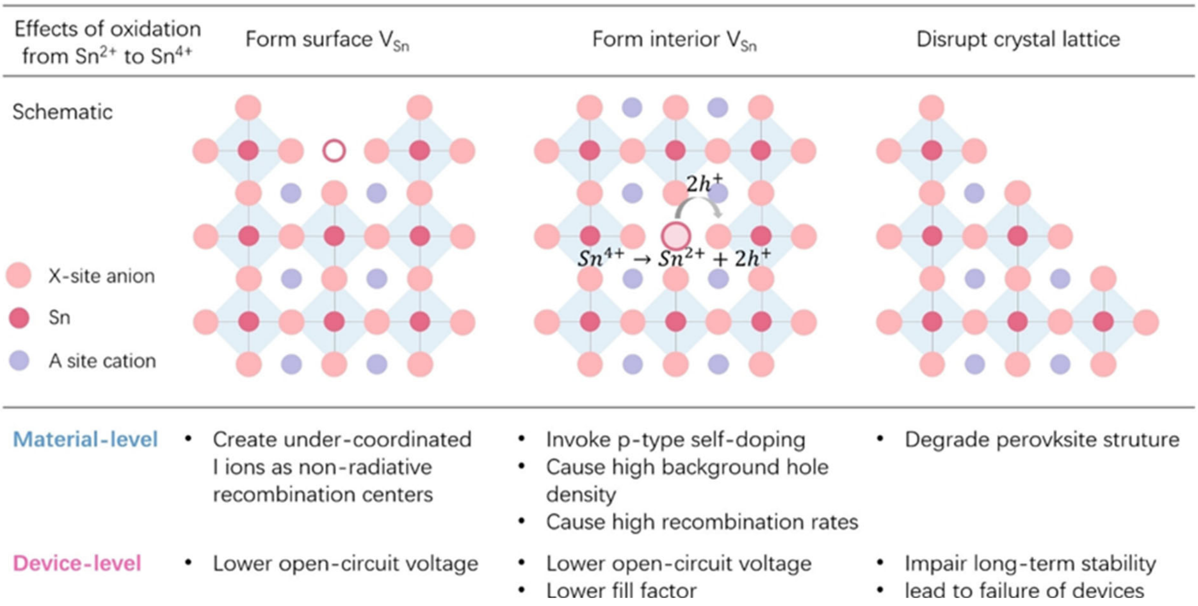

Figure 7. Schematic diagram of the effect of Sn vacancies on materials and devices[36]

3. APPLICATION OF THP IN OPTOELECTRONIC DEVICES

3.1. Solar cells

Typically, solar cells (PSCs) that incorporate perovskite compounds as the light-harvesting active layer are referred to as perovskite solar cells. These cells use organic or inorganic materials as the active layer, with an electron transport layer (ETL) and a hole transport layer (HTL) on either side to facilitate charge transfer between the perovskite and the external circuit, thereby meeting performance requirements. Doping perovskite and its precursor solutions to mitigate Sn vacancy defects has been a widely used strategy to passivate defects and enhance the performance and stability of PSCs.

3.1.1 TBA doping

Li et al. [27] used a small amount of 2D tetrabutylammonium (TBA) cations to passivate Sn-based perovskite films. The incorporation of TBA cations improved surface coverage, inhibited Sn^{2+} oxidation, and reduced background carrier density. This led to significant enhancements in device performance, with PCEs of $FASnI_3$ increasing from 4.0% to 7.0% and $CsSnI_3$ from 1.3% to 2.8%.

3.1.2 Multi-Component Optimization

Zhang et al. [57] developed a combined PMPS and DPPS approach, integrating precursor doping, antisolvent modification, and surface passivation to enhance Sn-based PSC performance. The PMPS-treated devices exhibited improved stability and achieved a PCE of 14.18%. Characterization revealed that PMPS played a crucial dual-functional role: its passivation effect significantly smoothed the film morphology and increased grain size, improving Jsc. Additionally, its ability to reduce Sn^{4+} and modulate surface energy levels contributed to an enhanced Voc, leading to overall performance improvements.

3.1.3 Design of Alternative HTLs

Yan et al. [52] designed a new molecular structure based on DBTDO as the core, combined with donor units TPA and DTPA as peripheral groups, to synthesize alternative HTL materials. The TPA-DBTDO-DTPA HTM formed smoother films that supported the growth of a dense perovskite layer and optimized energy level alignment. Its sulfonyl groups effectively passivated buried defects in the perovskite, enhancing the open-circuit voltage (Voc) of Sn-Pb hybrid PSCs. Using this HTL, the PSC achieved a PCE of 22.6% and maintained 75.9% of its initial efficiency after 1000 hours of aging in a nitrogen environment, significantly outperforming the PEDOT:PSS-based control devices, as shown in Figure 8(a).

3.1.4 CsAc Doping

Li et al. [29] introduced cesium acetate (CsAc)-doped PEDOT:PSS as an HTL during the crystallization process of tin-based perovskites. The CsAc doping induced preferential crystal orientation, increased grain size, and improved the crystallization quality of the perovskite layer. It also enhanced the conductivity of PEDOT:PSS and improved the wettability of the perovskite precursor solution, strengthening the interface contact between the HTL and the perovskite layer. As a result, CsAc doping increased the average Jsc from 23.80 mA cm^{-2} to 27.60 mA cm^{-2}, achieving a PCE of 10.99%, as shown in Figure 8(b).

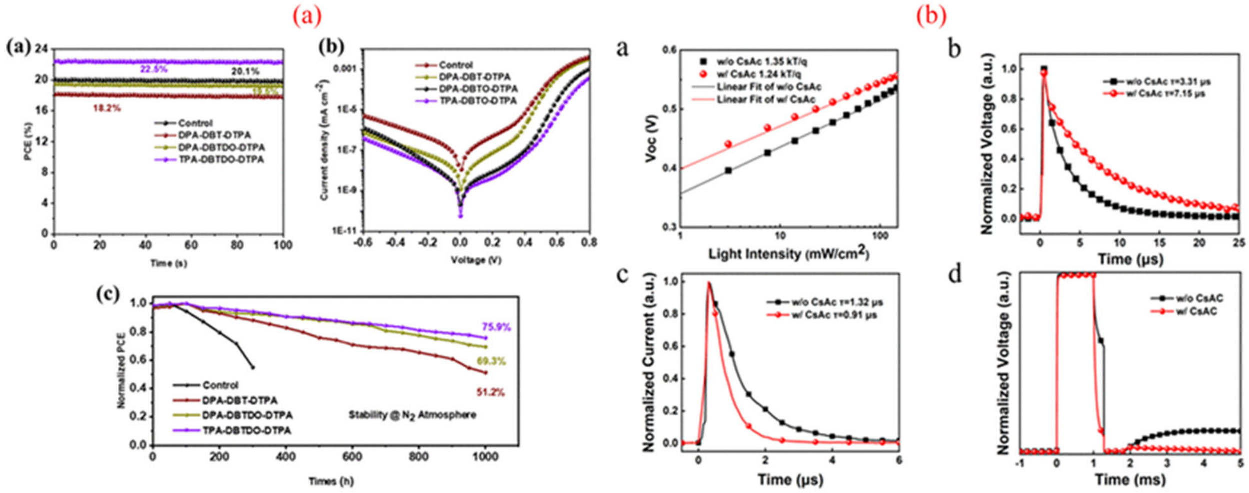

Figure 8. (a) Optimal conversion efficiency, dark J-V curve and long-term stability under N_2 line of tin-based perovskite PSCs prepared by DPA and TPA-doped PEDOT:PSS (b) EQE spectra, light-dependent Voc, transient photovoltage, and photocurrent response spectra under CsAc-doped HTL

3.2. Photodetectors

Perovskites with their broad-spectrum light absorption, are widely used not only in solar cells but also in photodetectors (PDs) for ultraviolet (UV), visible, near-infrared (NIR), and X-ray detection. Unlike solar cells, PDs do not require the optimization of HTL and ETL. Instead, they rely on fabricating electrodes with specific channel distances on the surface and applying voltage for light detection[49]. Enhancing perovskite PD performance mainly involves high-quality perovskite thin films、nanostructured perovskites、perovskite quantum dots (QDs) and improving perovskite stability. This section discusses representative methods for improving Sn-based perovskite PD performance based on the above approaches.

3.2.1 Solvent Dissolution Method

Zhang et al. [56] developed a simple and cost-effective method to improve the stability of Cs_2SnI_6 by dissolving Cs_2SnI_6 powder in anhydrous ethanol, n-hexane, deionized water, or DMF to fabricate PDs. The ethanol dissolution method resulted in the best performance, achieving a responsivity of 8.53 A/W and a detectivity of 8.87×10^{11} Jones under 405 nm laser illumination.

3.2.2 CsF Additive Engineering

Zhang et al. [58] proposed a dual-functional CsF (cesium fluoride) additive treatment to enhance the quality and optoelectronic performance of $FASnI_3$ perovskite films. With a CsF doping concentration of 15%, the responsivity of the fabricated PD increased by over 60 times compared to the undoped device. Cs^+ substitution and F^- additive effects synergistically inhibited Sn^{2+} oxidation, optimized crystal growth, and passivated defects.

3.2.3 Seed-Assisted Solution Growth

In 2024, Gao et al. [15] pioneered the seed-assisted solution growth (SSG) strategy to fabricate high-quality, lead-free $FASnI_3$ quasi-single-crystal (QSC) thick films. By uniformly distributing $FASnI_3$ seed crystals on the substrate and introducing a saturated $FASnI_3$ solution in γ-butyrolactone (GBL), dense and continuous films were successfully formed. The PD based on this QSC $FASnI_3$ thick film demonstrated a red-light detectivity of 1.0×10^{10} Jones at a low bias of 0.1 V, showcasing excellent self-powered detection capability. As shown in Figure 9(b), this study marks the first successful fabrication of a large-area (1 × 1 cm^2) continuous, high-quality, lead-free Sn-based QSC thick film, paving the way for the development of various Sn-based optoelectronic devices and representing a significant milestone in the field of tin-based perovskites.

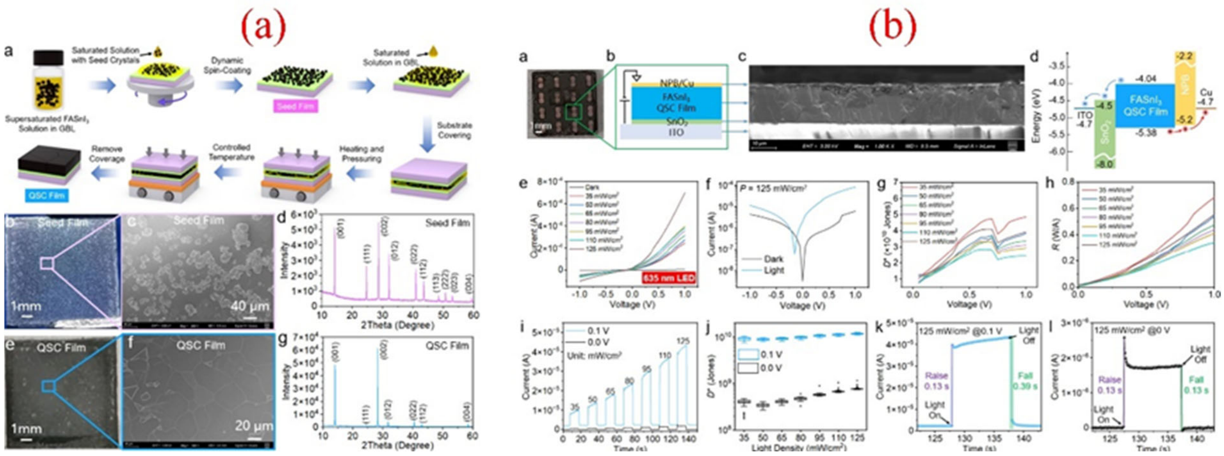

Figure 9. (a) Schematic diagram of the flow of the SSG method and SEM images and XRD spectra of the $FASnI_3$ single crystal film (b) Photos, energy level maps, and performance characterization of the PD based on the $FASnI_3$ single crystal film

3.3. Light-emitting diodes

In addition to solar cells and photodetectors, halide perovskites are also commonly used as excellent light-emitting materials and have been applied in the fabrication of light-emitting diodes (LEDs) [6; 60]. The structure of LEDs is similar to that of solar cells, with the perovskite acting as the light-emitting layer instead of the light-absorbing layer. HTL and ETL are fabricated on either side to ensure unidirectional charge transport. When powered, electrons and holes recombine radiatively in the perovskite emission layer, promoting light emission[13]. This section will focus on improving the stability of tin-based perovskites, highlighting recent advancements in achieving new highs in external quantum efficiency for tin-based perovskite LEDs.

3.3.1 Anti-Oxidation Strategy for $CsSnI_3$

Guan et al. [18] proposed an anti-oxidation strategy for $CsSnI_3$, which involves triggering hydrolysis of tin tetrahalides in the presence of moisture to selectively eliminate defects induced by Sn^{4+}, while maintaining the stability of Sn^{2+} in the $CsSnI_3$ film. Based on this strategy, the research team successfully fabricated a second NIR window LED with an emission wavelength of 945 nm, achieving a performance breakthrough with an EQE of 7.6% and a device lifetime extended to 82.6 hours. This study provides an effective method for enhancing the stability of tin-based perovskite optoelectronic devices and contributes to the development of high-performance NIR electronic devices.

3.3.2 High Stability Tin-Based Perovskite Nanocrystals

Yang et al. [53] reported highly stable tin-based perovskite nanocrystals, which were synthesized using tin acetate as the Sn^{2+} source to enhance the stability of the Sn−O bond and effectively suppress the oxidation of Sn^{2+}, resulting in Cs_xSnBr_{x+2}@CsBr ($1 < x < 4$) perovskite nanocrystals. This material demonstrated a high PLQY of 78.2% and exceptional environmental stability. PLQY lifetime tests showed that the nanocrystals maintained stability for 1287 hours under ambient conditions, and the stability was extended to 2200 hours in a nitrogen atmosphere, significantly outperforming traditional tin-based perovskite materials. This research provides an effective strategy for constructing highly stable tin-based perovskite nanocrystals and demonstrates their potential applications in high-performance white LEDs.

3.3.3 Interface Engineering with Ammonium Thiocyanate (NH_4SCN)

Li et al. [28] employed ammonium thiocyanate (NH_4SCN) to modify the HTL and effectively regulate the rapid crystallization process of tin-based perovskite through interface engineering, significantly improving the stability of tin halide perovskite thin films. The study showed that thiocyanate ions (SCN^-) in the PEDOT:PSS interacted with the Sn-I framework, which not only reduced the crystallization rate of the perovskite but also effectively suppressed the oxidation of Sn^{2+} while passivating defects caused by under-coordinated Sn^{2+}. The optimized tin-based perovskite thin films exhibited a smoother morphology, higher uniformity, and a more compact structure, effectively reducing Sn^{4+}-related defect states, thereby enhancing radiative recombination efficiency. Thanks to this strategy, the tin-based PeLED device achieved a peak EQE of 5.8%, approximately 4.6 times higher than the unmodified control device, as shown in Figure 10. This research indicates that rational interface engineering to control crystallization dynamics not only improves the quality and stability of tin-based perovskite thin films but also provides an important optimization pathway for the development of high-efficiency tin-based PeLEDs.

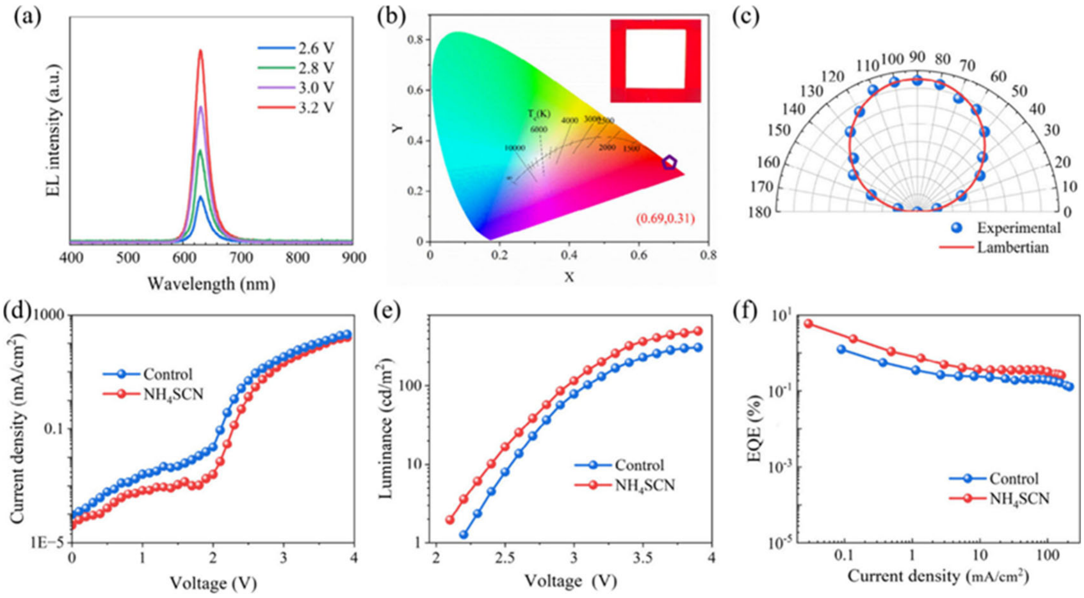

Figure 10. (a) EL spectra at different voltages. (b) CIE coordinate system. (c) Measurement of EL intensity as a function of angle. (d) J-V curves, (e) brightness-voltage curves, and (f) EQE-current density curves of the experimental and control groups.

4. SUMMARY AND OUTLOOK

This article provides a systematic summary of the structure, properties, and recent advancements of tin-based perovskites in optoelectronic devices. However, compared to lead-based perovskites, tin-based perovskites face more severe environmental stability challenges, primarily due to the oxidation of Sn^{2+} to Sn^{4+}, which leads to material degradation and device performance degradation. Therefore, improving the environmental stability of tin-based perovskites is key to driving their commercialization. Overall, the development of tin-based perovskites is progressing rapidly and diversely, but it is still in the breakthrough phase. The improvement in the performance of optoelectronic devices is mainly reflected in defect passivation, additive stabilization, HTL and ETL interface engineering, energy level regulation, and structural optimization, along with research on nano- and low-dimensional perovskites. In the future, these methods can serve as supporting points to further enhance stability and device lifespan, thus promoting their commercialization in fields such as flexible electronics, photodetectors, and lead-free photovoltaics. With the continuous advancement of new stabilization strategies, tin-based perovskites are expected to become the next generation of efficient and environmentally friendly optoelectronic materials, providing significant support for the development of sustainable energy and optoelectronic technologies.

REFERENCES

[1] J (2021), "A stand out family", Nature Materials. vol. 20, no. 10, pp. 1303-1303.

[2] Antonio Abate J (2017), "Perovskite Solar Cells Go Lead Free", Joule. vol. 1, no. 4, pp. 659-664.

[3] Muhammad Awais, et al. J (2021), "Tin Halide Perovskites Going Forward: Frost Diagrams Offer Hints", ACS Materials Letters. vol. 3, no. 3, pp. 299-307.

[4] James M. Ball and Annamaria Petrozza J (2016), "Defects in perovskite-halides and their effects in solar cells", Nature Energy. vol. 1, no. 11, p. 16149.

[5] H. Cao, et al. J (2021), "The effect of defects in tin-based perovskites and their photovoltaic devices", Materials Today Physics. vol. 21, p. 100513.

[6] Y. Cao, et al. J (2018), "Perovskite light-emitting diodes based on spontaneously formed submicrometre-scale structures", (in eng), Nature. vol. 562, no. 7726, pp. 249-253.

[7] Chun-Hao Chen, et al. J (2023), "Toxicity, Leakage, and Recycling of Lead in Perovskite Photovoltaics", Advanced Energy Materials. vol. 13, no. 14, p. 2204144.

[8] Sheng Chen, et al. J (2019), "First-principles study on the electronic properties of perovskites MASnaPb(1 − a)XbY(3 − b) (X, Y = Cl, Br, I)", Results in Physics. vol. 14, p. 102408.

[9] In Chung, et al. J (2012), "CsSnI3: Semiconductor or Metal? High Electrical Conductivity and Strong Near-Infrared Photoluminescence from a Single Material. High Hole Mobility and Phase-Transitions", Journal of the American Chemical Society. vol. 134, no. 20, pp. 8579-8587.

[10] E. Lora da Silva, et al. J (2015), "Phase stability and transformations in the halide perovskite ${\mathrm{CsSnI}}_{3}$", Physical Review B. vol. 91, no. 14, p. 144107.

[11] Linjie Dai, et al. J (2021), "Slow carrier relaxation in tin-based perovskite nanocrystals", Nature Photonics. vol. 15, no. 9, pp. 696-702.

[12] Margaret Dawson, et al. J (2022), "A Review of Three-Dimensional Tin Halide Perovskites as Solar Cell Materials", Materials Research.

[13] Azhar Fakharuddin, et al. J (2022), "Perovskite light-emitting diodes", Nature Electronics. vol. 5, no. 4, pp. 203-216.

[14] Weiyin Gao, et al. J (2019), "Interface Engineering in Tin Perovskite Solar Cells", Advanced Materials Interfaces. vol. 6, no. 24, p. 1901322.

[15] Weiyin Gao, et al. J (2024), "Seed-Crystal-Assisted Space-Confined Growth of FASnI3 Quasi-Single-Crystal Thick Films and Their Photodetection Characteristics", ACS Energy Letters. vol. 9, no. 10, pp. 5045-5055.

[16] Nadja Glück and Thomas Bein J (2020), "Prospects of lead-free perovskite-inspired materials for photovoltaic applications", Energy & Environmental Science. 10.1039/D0EE01651A vol. 13, no. 12, pp. 4691-4716.

[17] Anuj Goyal, et al. J (2018), "Origin of Pronounced Nonlinear Band Gap Behavior in Lead–Tin Hybrid Perovskite Alloys", Chemistry of Materials. vol. 30, no. 11, pp. 3920-3928.

[18] Xiang Guan, et al. J (2024), "Targeted elimination of tetravalent-Sn-induced defects for enhanced efficiency and stability in lead-free NIR-II perovskite LEDs", Nature Communications. vol. 15, no. 1, p. 9913.

[19] Xianyuan Jiang, et al. J (2021), "Tin Halide Perovskite Solar Cells: An Emerging Thin-Film Photovoltaic Technology", Accounts of Materials Research. vol. 2, no. 4, pp. 210-219.

[20] Efat Jokar, et al. J (2023), "Emerging Opportunities in Lead-Free and Lead–Tin Perovskites for Environmentally Viable Photodetector Applications", Chemistry of Materials. vol. 35, no. 9, pp. 3404-3426.

[21] Dianxing Ju, et al. J (2018), "Tunable Band Gap and Long Carrier Recombination Lifetime of Stable Mixed CH3NH3PbxSn1–xBr3 Single Crystals", Chemistry of Materials. vol. 30, no. 5, pp. 1556-1565.

[22] V. Kanchana, et al. J (2024), "Computational Advances for Energy Conversion: Unleashing the Potential of Thermoelectric Materials", Solid State Sciences.

[23] Jin Young Kim, et al. J (2020), "High-Efficiency Perovskite Solar Cells", Chemical Reviews. vol. 120, no. 15, pp. 7867-7918.

[24] Geneva Laurita, et al. J (2017), "Chemical tuning of dynamic cation off-centering in the cubic phases of hybrid tin and lead halide perovskites", CHEMICAL SCIENCE. 10.1039/C7SC01429E vol. 8, no. 8, pp. 5628-5635.

[25] Lei Lei, et al. J (2021), "Metal Halide Perovskites for Laser Applications", ADVANCED FUNCTIONAL MATERIALS. vol. 31, no. 16, p. 2010144.

[26] Bo Li, et al. J (2020), "Tin-Based Defects and Passivation Strategies in Tin-Related Perovskite Solar Cells", ACS Energy Letters. vol. 5, no. 12, pp. 3752-3772.

[27] Junming Li, et al. J (2020), "Enhanced Performance of Sn-Based Perovskite Solar Cells by Two-Dimensional Perovskite Doping", ACS Sustainable Chemistry & Engineering. vol. 8, no. 23, pp. 8624-8628.

[28] Li Li, et al. J (2025), "Optimizing the Hole-Transport Layer with Ammonium Thiocyanate for Enhanced Performance in Lead-Free Perovskite Light-Emitting Diodes", ACS Applied Electronic Materials.

[29] Xiaomeng Li, et al. J (2024), "Efficient Tin-Based Perovskite Solar Cell with a Cesium Acetate Pre-buried PEDOT:PSS Hole Transport Layer", The Journal of Physical Chemistry Letters. vol. 15, no. 5, pp. 1355-1362.

[30] Joseph S. Manser, et al. J (2016), "Intriguing Optoelectronic Properties of Metal Halide Perovskites", Chemical Reviews. vol. 116, no. 21, pp. 12956-13008.

[31] Xin Mao, et al. J (2018), "First-Principles Screening of All-Inorganic Lead-Free ABX3 Perovskites", Journal of Physical Chemistry C. vol. 122, pp. 7670-7675.

[32] D. Meggiolaro, et al. J (2020), "Tin versus Lead Redox Chemistry Modulates Charge Trapping and Self-Doping in Tin/Lead Iodide Perovskites", (in eng), J Phys Chem Lett. vol. 11, no. 9, pp. 3546-3556.

[33] Rubaiya Murshed, et al. J (2023), "SnF2-Doped Cs2SnI6 Ordered Vacancy Double Perovskite for Photovoltaic Applications", Solar RRL. vol. 7, no. 19, p. 2300165.

[34] Sanjay Pachori, et al. J (2022), "Fundamental Physical Properties of Nontoxic Tin-Based Formamidinium FASnX3 (X = I, Br, Cl) Hybrid Halide Perovskites: Future Opportunities in Photovoltaic Applications", Energy Technology. vol. 10, no. 2, p. 2100709.

[35] Elizabeth S. Parrott, et al. J (2016), "Effect of Structural Phase Transition on Charge-Carrier Lifetimes and Defects in CH3NH3SnI3 Perovskite", The Journal of Physical Chemistry Letters. vol. 7, no. 7, pp. 1321-1326.

[36] Damiano Ricciarelli, et al. J (2020), "Instability of Tin Iodide Perovskites: Bulk p-Doping versus Surface Tin Oxidation", ACS Energy Letters. vol. 5, no. 9, pp. 2787-2795.

[37] David E. Scaife, et al. J (1974), "Crystal preparation and properties of cesium tin(II) trihalides", Journal of Solid State Chemistry. vol. 9, no. 3, pp. 308-314.

[38] Tejas S. Sherkar, et al. J (2017), "Recombination in Perovskite Solar Cells: Significance of Grain Boundaries, Interface Traps, and Defect Ions", ACS Energy Letters. vol. 2, no. 5, pp. 1214-1222.

[39] Constantinos C. Stoumpos, et al. J (2013), "Semiconducting Tin and Lead Iodide Perovskites with Organic Cations: Phase Transitions, High Mobilities, and Near-Infrared Photoluminescent Properties", Inorganic Chemistry. vol. 52, no. 15, pp. 9019-9038.

[40] Yukari Takahashi, et al. J (2011), "Charge-transport in tin-iodide perovskite CH3NH3SnI3: origin of high conductivity", Dalton Transactions. 10.1039/C0DT01601B vol. 40, no. 20, pp. 5563-5568.

[41] Shuxia Tao, et al. J (2019), "Absolute energy level positions in tin- and lead-based halide perovskites", Nature Communications. vol. 10, no. 1, p. 2560.

[42] Paolo Umari, et al. J (2014), "Relativistic GW calculations on CH3NH3PbI3 and CH3NH3SnI3 Perovskites for Solar Cell Applications", Scientific Reports. vol. 4, no. 1, p. 4467.

[43] Hiroki Uratani and Koichi Yamashita J (2017), "Charge Carrier Trapping at Surface Defects of Perovskite Solar Cell Absorbers: A First-Principles Study", The Journal of Physical Chemistry Letters. vol. 8, no. 4, pp. 742-746.

[44] Haiyan Wang, et al. (2022). A Review of Perovskite-Based Photodetectors and Their Applications. In NANOMATERIALS.

[45] Mei Wang, et al. J (2020), "Systematic optimization of perovskite solar cells via green solvent systems", Chemical Engineering Journal. vol. 387, p. 123966.

[46] Ning Wang, et al. J (2016), "Heterojunction-Depleted Lead-Free Perovskite Solar Cells with Coarse-Grained B-γ-CsSnI3 Thin Films", Advanced Energy Materials. vol. 6, no. 24, p. 1601130.

[47] Bo Wu, et al. J (2017), "Long Minority-Carrier Diffusion Length and Low Surface-Recombination Velocity in Inorganic Lead-Free CsSnI3 Perovskite Crystal for Solar Cells", ADVANCED FUNCTIONAL MATERIALS. vol. 27, no. 7, p. 1604818.

[48] Lian Xiao, et al. J (2023), "On biosafety of Sn-containing halide perovskites", Energy & Environmental Science. 10.1039/D2EE02510H vol. 16, no. 5, pp. 2120-2132.

[49] Wei-Long Xu, et al. J (2024), "Tin-based perovskite films fabricated by chemical vapor deposition for photodetector application", Chemical Physics. vol. 580, p. 112213.

[50] Koji Yamada, et al. J (1991), "Structural phase transitions of the polymorphs of CsSnI3 by means of rietveld analysis of the X-ray diffraction", Chemistry Letters. vol. 20, pp. 801-804.

[51] Koji Yamada, et al. J (1998), "Phase Transition and Electric Conductivity of ASnCl3 (A = Cs and CH3NH3)", Bulletin of the Chemical Society of Japan. vol. 71, pp. 127-134.

[52] Meng Yan, et al. J (2024), "Small Molecular Dibenzo[b,d]thiophene-Based Hole Transport Materials for Tin–Lead Perovskite Solar Cell", The Journal of Physical Chemistry Letters. vol. 15, no. 44, pp. 11119-11125.

[53] Shuang Yang, et al. J (2023), "Superstable CsxSnBrx+2@CsBr Nanocrystals with Over 1200 h of Half-Value PLQY in Air", ACS Applied Materials & Interfaces. vol. 15, no. 30, pp. 36716-36723.

[54] Wan-Jian Yin, et al. J (2014), "Unusual defect physics in CH3NH3PbI3 perovskite solar cell absorber", Applied Physics Letters. vol. 104, no. 6, p. 063903.

[55] Chunqian Zhang, et al. (2024). A Systematical Study on Bands and Defects of CsBX3 (B = Pb, Sn, Ge, X = Cl, Br, I) Perovskite Based on First Principles. In Molecules.

[56] Jingjing Zhang, et al. J (2024), "Preparation of Cs2SnI6 perovskite thin films based on solvent engineering and their properties of photodetectors", Sensors and Actuators A: Physical. vol. 378, p. 115798.

[57] Zheng Zhang, et al. J (2024), "Over 14% efficiency of highly reproducible Sn perovskite solar cell via defect passivation and morphology repairment", Chemical Engineering Journal. vol. 483, p. 149345.

[58] Zhihang Zhang, et al. J (2024), "Performance Enhancement of Tin-Based Perovskite Photodetectors through Bifunctional Cesium Fluoride Engineering", ACS Applied Materials & Interfaces. vol. 16, no. 10, pp. 12773-12780.

[59] Zhihao Zhang, et al. J (2023), "Mechanistic Understanding of Oxidation of Tin-based Perovskite Solar Cells and Mitigation Strategies", Angewandte Chemie International Edition. vol. 62, no. 45, p. e202308093.

[60] Lin Zhu, et al. J (2021), "Unveiling the additive-assisted oriented growth of perovskite crystallite for high performance light-emitting diodes", Nature Communications. vol. 12, no. 1, p. 5081.